Multilayers Consisting of Oriented Charged α-Helical Polypeptides

*Martin Müller,**[1] *Thomas Reihs,*[1] *Bernd Kessler,*[1] *Hans-Jürgen Adler,*[2] *Klaus Lunkwitz*[1]

[1] Institute of Polymer Research Dresden e.V. (IPF), Hohe Strasse 6, D-01069 Dresden, Germany
E-mail: mamuller@ipfdd.de
[2] Institute of Macromolecular and Textile Chemistry, Technical University Dresden (TUD), Mommsenstrasse 13, D-01062 Dresden, Germany

Summary: Polyelectrolyte Multilayers (PEMs) consisting of cationic α-helical poly(L-lysine) (PLL) and optionally anionic poly(vinysulfate) (PVS) (i) or α-helical poly(L-glutamic acid) (PLG) (ii) were deposited at substrates texturized by parallel nanoscopic surface grooves, respectively. Using dichroic Attenuated Total Reflexion Fourier Transform Infrared (ATR-FTIR) spectroscopy the consecutive deposition, conformation and macromolecular order of stiff polyelectrolytes within PEMs were studied. From the dichroic ratios of the Amide I and Amide II bands order parameters $S \geq 0.6$ ($S = 1$ for high, $S = 0$ for low order) were obtained suggesting a significant alignment of charged α-helical polypeptides in PEMs. For the PEM consisting of PLL/PVS the deposited amount as well as the order parameter S significantly depended on the molecular weight (contour length) of PLL. Furthermore, the related opening angle γ of a model cone consisting of α-helical PLL rods was proven to be a function of both contour length and width of the confining surface grooves. AFM pictures on PEM-PLL/PVS showed anisotropically oriented worm-like structures As a second system PEMs of PLL and PLG, both in the α-helical conformation, are introduced. A high order parameter of both spectroscopically indistinguishable polypeptides was found. A model of aligned rod/coil (i) and rod/rod (ii) structures was proposed. Finally, multilayers of stiff conductive polymers like polyaniline (PANI) alternating with poly(acrylic acid) (PAC) are introduced. Preliminary results on their deposition and alignment are given.

Keywords: dichroic ATR-FTIR spectroscopy; multilayers; orientation; polyelectrolytes; polypeptides

Introduction

Polyelectrolyte multilayers (PEMs) consecutively adsorbed on solid substrates, which were initiated by Decher,[1] go back to polyelectrolyte complexes (PECs) formed by mixing oppositely charged polyelectrolytes in the solution shown e.g. by Michaels and Kabanov.[2,3] PEMs and PECs have gained much interest in the last decade, since they allow for defined nanoarchitectures and selective surface modification and are challenging objects for

 DOI: 10.1002/masy.200450715

polyelectrolyte theory. In the beginning PEMs were claimed to be composed of stratified individual layers. However this model was replaced by another one, according to which commonly used flexible polyelectrolytes cause high entanglement, no distinct layering and a low degree of order in the internal structure.[4, 5] Nevertheless, the generation of PEMs consisting of stratified or lamellar arranged PEL layers is an interesting obective. Macromolecular order in PEMs can be achieved by several concepts: Besides PEMs composed of layered silicates alternating with polyactions[6] (i), those composed of hydrophobic ionenes[7] have been used (ii). As a third concept PEMs composed of charged stiff α-helical polypeptides alternating with oppositely charged strong polyanions or polycations, respectively, were introduced therein[8, 9] (iii) and shall be reviewed and extended here.

Generally, PEMs consisting of charged polypeptides are subjects of fundamental structural studies[8, 9, 10, 11, 12] as well as for biomedical and pharmaceutical applications, which was shown therein.[13, 14, 15, 16] Furthermore, PEMs exposing those polypeptides in both defined conformations and orientations might be a new strategy for biomimetic surface modification as will be shown therein.[17] In that framework PEMs consisting of *in-plane* oriented α-helical polypeptides are expected to bind specifically α-helical rich proteins ´side on´, which may be not the case for α-helical polypeptides assembled normal to the substrate or for immobilized polypeptides in other conformations (β-sheet, random coil).

Experimental

Polyelectrolytes

For the consecutive deposition of stiff charged polypeptides alternating with oppositely charged polyelectrolytes (PELs) poly(L-lysine) (PLL, M_w = 3 400, 20 700, 25 700, 57 900, 80 000, 189 400, 205 000, 246 000, 309 500 g/mol, further denoted as ´PLL-3 400 – PLL-309 500´, SIGMA-ALDRICH) were combined optionally with poly(vinylsulfate) (PVS, M_w = 162 000 g/mol, POLYSCIENCE) or poly(L-glutamic acid) (PLG, M_w = 70 000 g/mol, SIGMA ALDRICH). All commercial polyelectrolyte samples were used without further purification. PLL, PVS, PLG and PDADMAC were dissolved in Millipore water or in 1 M $NaClO_4$ solution (MERCK, Darmstadt) at PEL concentrations c_{PEL} = 0.01 M. Polyaniline (PANI, PANIPOL, Finland) was dissolved in a mixture of water (pH = 4)/N-methyl-pyrrolidone (NMP) (9:1, v/v) yielding a concentration c_{PANI} = 0.001 M. Poly(acrylic acid) (PAC) was dissolved in water at c_{PAC} = 0.001 M and pH = 4.

Surfaces

The silicon substrates were cleaned[19] and texturized by mechanical treatment[8] as previously reported.

ATR-FTIR spectroscopy

The monitoring of consecutive deposition of the polyelectrolytes and the characterization of the deposited PEMs was performed by in-situ-ATR-FTIR spectroscopy using the SBSR concept[18] to obtain well compensated ATR-FTIR spectra, as it is described therein.[19] Dichroic measurements and data analysis were performed according to a methodology reported therein.[8] IR light was polarized by a wire grid polarizer (SPECAC, UK). The ATR-FTIR attachment was operated on the IFS 55 Equinox spectrometer (BRUKER-Saxonia, Leipzig) equipped with globar source and MCT detector. Typically polycation, rinsing (1 M $NaClO_4$) and polyanion solutions were stepwise injected by syringes in the *in-situ* measuring cell (IPF Dresden, M.M.) each step having a residence time of 15 min. p- and s-polarized ATR-FTIR spectra were recorded after each rinsing step, for which 200 scans were accommodated. To check for undesired time dependent variations the polarized spectra (p, s) were recorded in the sequence ´p - s – p´ and the first p-polarized spectrum was compared with the second one. No spectral differences should appear between the two p-polarized spectra. Either peak intensities or integrated band areas were used for the dichroic ratio determination of the amide bands.

Results and Discussion

In the following deposition and orientation data on the two consecutive polyelectrolyte multilayer (PEM) systems composed of 1. PLL/PVS and 2. PLL/PLG are presented. The influence of parameters like molecular weight (M_w), layer number z and of drying will be considered. Briefly deposition results on the PEM consisting of PANI/PAC (3.) are shown.

1. PEM of PLL/PVS

In Figure 1 typical ATR-FTIR spectra on the consecutively adsorbed PEMs (PEM-1 to PEM-5) of PLL/PVS in the presence of 1 M $NaClO_4$ are shown with increasing adsorption steps z from bottom to top. An increasing negative signal of the ν(OH) at about 3 400 cm^{-1} is visible, which is due to the removal of water from the surface upon PEM deposition, which is further commented on therein[20] Additionally, the increasing signals of the Amide I and Amide II

band at 1 650 and 1 550 cm^{-1}, due to the peptide groups of PLL, are also related to the PEM growth. The wavenumber positions of both amide bands suggest the α-helical conformation of the PLL component, as it is well known[21] Furthermore, the ν(O=S=O) signal around 1 230 cm^{-1} shows also increasing intensity with the adsorption step due to the PVS compound. The courses of these three bands are summarized in Figure 2. As we have shown previously[20] increasing polymer band (e.g. ν(CH), ν(C=O)) intensities A in multilayered systems scale with a function of the type A(z) = 1 - exp(-L*z) (L: thickness parameter, z: adsorption steps), whereas the increase of the negative ν(OH) band scales with a function of the type A(z) = exp(L*z) - 1. A slight indication of a zig-zag-like course is seen in all three curves, which can be explained by a certain removal of the last adsorbed PEL layer by the following one. For example after all PLL steps (odd) in the next step (PVS, even) the PLL amount, as seen by the amide band integrals, drops a little bit down. This is also observed for the water removal monitored by the negative ν(OH) band integral. Since in the PLL steps the higher negative ν(OH) band increase was observed compared to the previous PVS steps, respectively, PLL seems to form thicker incremental adsorption layers than PVS.

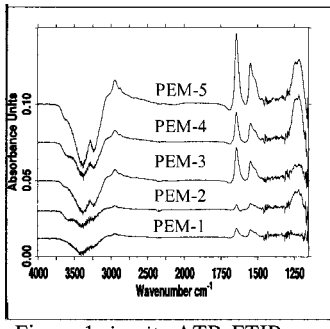

Figure 1. *in-situ* ATR-FTIR spectra on the consecutive deposition of PLL (205.000 g/mol) and PVS (162.000 g/mol) at Si-crystals (IRE) in the presence of 1 M $NaClO_4$ (unpolarized spectra of PEM-1 to PEM-5).

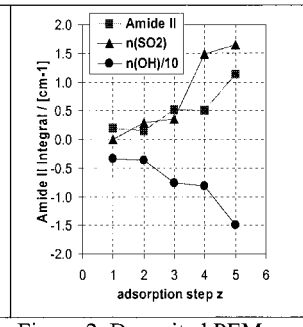

Figure 2. Deposited PEM amount during consecutive adsorption of PLL/PVS (1 M $NaClO_4$) in dependence of the adsorption step z rationalized by the Amide II, ν(O=S=O) and negative ν(OH) band (related to Figure 1).

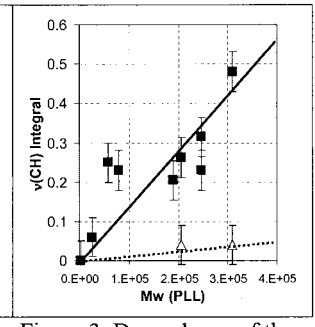

Figure 3. Dependence of the deposited PEM amount on the PLL molecular weight (M_w= 3.400 - 309.000 g/mol) for $NaClO_4$ (full line) and salt free preparation (dotted line).

In Figure 3 the the deposited amount of PEM-5 of PLL/PVS is shown in dependence of the PLL molecular weight (M_w) for the salt free and the $NaCLO_4$ containing system. Qualitatively, the larger adsorbed amount increase of the PEM-5 of PLL/PVS was obtained in

the presence of 1 M $NaClO_4$ compared to the lower one for the salt free system. This is due to both the salt screening effect (i) and the different conformations of PLL (ii). (i) Firstly, PLL in the absence of salt is highly charged, which favors electrostatic attraction to the respective oppositely charged surface in all adsorption steps. However if saturation is reached in every respective adsorption step, further PLL adsorption is prevented by electrostatic repulsion. This is not the case for PLL in the presence of $NaClO_4$, since electrostatic interactions are screened by the high salt concentration (1 M) preventing repulsion. Additionally PVS in the presence of 1 M $NaClO_4$ adopts the more coiled conformation, which might also contribute to the higher PEM adsorbed amount. In this case the PVS coils might act as weak binders between the assembled PLL rods. In how far at that ionic strength electrostatic contributions may play a role at all, has to be treated by theoretical approaches, but can not speculated on here. (ii) Secondly, PLL in the absence of salt is in the random coil conformation and PLL in the presence of $NaCL0_4$ is in the α-helical state and forms a rod. From thermodynamic considerations ($\Delta G = \Delta H - T\Delta S$) rods loose less entropy after adsorption onto surfaces than coils, since the rod conformation does not change ($\Delta S \approx 0$) so much when adsorbed at the surface compared to the conformation of coils loosing degrees of freedom upon surface spreading ($\Delta S < 0$). Furthermore, the enthalpy contribution of rods self-assembling in-plane at the surface (forming a kind of crystal structure) might be higher ($\Delta H < 0$) compared to the enthalpic contribution of coils, which can not show such assembly or cooperative stabilization.

PLL/PVS orientation

Access to the PLL orientation within PEMs can be obtained via dichroic ATR-FTIR spectroscopy, as it is shown in Fig. 4a and 4b. In previous publications[8, 9] we have already shown, that on texturized Si substrates α-helical PLL-205.000 could be oriented along the surface grooves, whereas on untexturized ones this was not the case. Hence texturization was found to be crucial for polymer orientation. Based on these findings texturized substrates are focussed in that report in order to study further parameters of this alignment effect like molecular weight (M_w) and layer number (adsorption step) z and additionally PEMs consisting of two α–helical polypeptides. In Figure 4a and Figure 4b p- and s-polarized spectra of the PEM-5 of PLL/PVS in the presence of $NaClO_4$ are shown for PLL with M_w = 25 700 g/mol (further denoted as PLL-25.700, Figure 4a) and 205 000 g/mol (further denoted as PLL-205.000, Figure 4b), respectively. Qualitatively, for PLL-205 000 a high dichroic effect was observed, i.e. the ratios with respect to the Amide I and the Amide II band were

differing very much. This was not the case for PLL-25.700, where the R_Y^{ATR} value of the Amide I was about the same of the Amide II. The dichroic ratios are summarized in the Table 1.

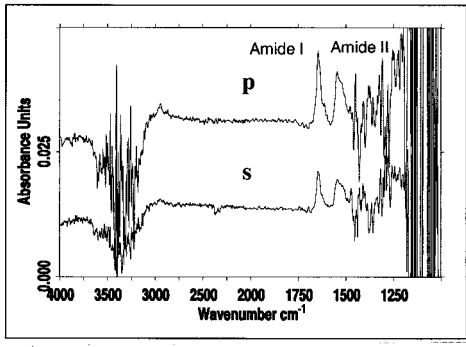

Figure 4a. p- and s-polarized ATR-FTIR spectra of the PEM-5 of PLL (25.700 g/mol) and PVS in the presence of 1 M $NaClO_4$.

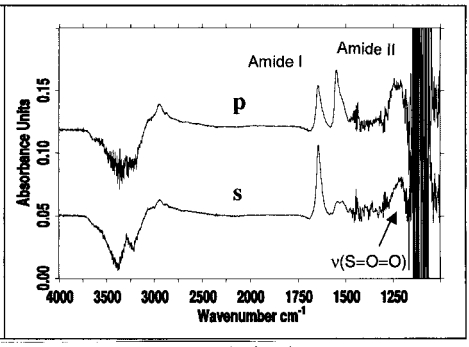

Figure 4b. p- and s-polarized ATR-FTIR spectra of the PEM-5 of PLL (205.000 g/mol) and PVS in the presence of 1 M $NaClO_4$.

Orientation analysis

For the quantitative analysis of dichroic ATR-IR data a formalism was applied developed by Zbinden and Fringeli[22, 23] at polymer and smaller liquid crystalline compounds and adapted to assembled α-helical polypeptide systems therein,[8, 9] for which the setup is shown in Figure 5a. The basic equation of dichroism[24] is given in the following:

$$A \propto \vec{E}^2 \bullet \vec{M}^2 \cos^2(\vec{E},\vec{M}) \tag{1}$$

Accordingly, a maximum absorbance A is obtained if the angle between the electric field vector E and the transition dipole moment M is 0° and minimum A is obtained if the angle is 90°. Experimentally, a polarizer with p- and s-setting is commonly used for the generation of polarized light with an electric field vector oscillating parallel or vertical with respect to the substrate normal, respectively. In eq. (2) the experimental dichroic ratio measured in the ATR mode R_y^{ATR} of A_p and A_s, which are the integrated absorbances of a given band measured with p- and with s-polarized light, is given.

$$R_y^{ATR} = \frac{A_p}{A_s} \tag{2}$$

For simplification R_y^{ATR}, the dichroic ratio measured in ATR mode, can be converted by Equation (3) into a dichroic ratio R^T, which would have been measured in transmission mode, knowing the amplitudes of the relative electric field components (E_x, E_y, E_z) of the evanescent wave (Figure 5b).

$$R^T = R_y^{ATR} \cdot \frac{E_y^2}{(E_x^2 + E_z^2)} \tag{3}$$

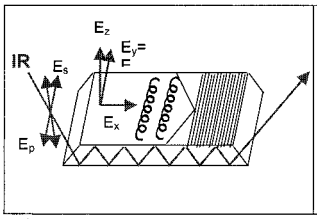

Figure 5a. (From [9], with kind permission of ACS). Experimental setup for dichroic ATR-IR measurements (ATR mode) on texturized (grooves) Si substrates.

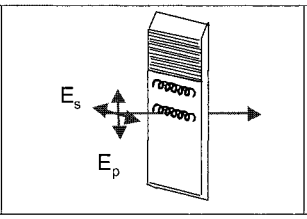

Figure 5b. Experimental setup for dichroic transmission IR measurements (transmission mode)

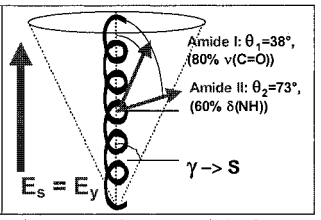

Figure 5c. Cone model of assembled and complexed PLL rods in the surface grooves [9].

Based on a cone model shown in Figure 5c from this R^T value an order parameter S can be calculated knowing the angle θ between the transition dipole moment M and the molecular main axis (e.g. the helical axis for polypeptides) according to Equation (4).

$$S = \frac{(1 - R^T)}{(2R^T + 1)} \cdot \frac{2}{(3\cos^2\theta - 1)} \tag{4}$$

Generally, values of S = 0 are obtained for no order, S = 1 for high order or parallel arrangements and of S = -1/2 for vertical arrangements with respect to a texture or a physical drawing direction, respectively. Since in a macromolecule R^T values can be determined for lots of vibration bands, a molecular model could be built based on their various relative transition dipole moment angles. Finally the above introduced order parameter S is directly related to the cone opening angle γ by Equation (5).

$$\gamma_0 = \arccos\left(\sqrt{\frac{2}{3}S + \frac{1}{3}}\right) \tag{5}$$

Accordingly, high values of γ correspond to low order parameters S or to a low degree of unidirectional alignment of the polymer rods.

For polypeptides the θ values for the Amide I and Amide II band and further for the Amide A band (around 3 300 cm^{-1}) are known from literature[25] according to which $\theta_{AMIDE\ A} = 28°$, $\theta_{AMIDE\ I} = 38°$, $\theta_{AMIDE\ II} = 73°$. The relative location and the angle of the transition dipole moment of the Amide I and Amide II band are depicted in Figure 5c. Hence, to determine the

order parameter of the polypeptide rods three independent informations can be used. The results for the PEM-5 of PLL/PVS are given in Table 1. Generally for IR spectra on PEMs in contact to water we take the order parameter S for the Amide II band as the reference value, since the Amide I band is slightly interfered by the δ(OH) band of water due to incomplete spectral compensation.

Table 1. Dichroic ratios R^T, order parameter S and opening angle γ for PEM-5 of PLL/PVS consisting of PLL with two different M_w.

	PLL-25.700/PVS		PLL-205.000/PVS	
	Amide I	Amide II	Amide I	Amide II
R^T	2.00	1.74	0.60	4.47
S	-0.19	0.10	0.79	0.75
γ	63°	51°	22°	24°

Dependence on the molecular weight M_w

As could be already seen from the dichroic ratios measured for the PLL-25 700 containing PEM-5 and the PLL-205 000 containing PEM-5, whose spectra are shown in Figure 4a and Figure 4b, different orientation level could be qualitatively concluded. Moreover in the Table 1 the order parameters S and cone opening angles γ determined by the equations (2) - (5) are given quantitatively. In Table 1 a significantly higher order parameter (S = 0.75 - 0.79) and thus higher degree of alignment of the PLL rods was obtained for the PLL-205.000 compared to the PLL-25 700 containing PEM (S = -0.19 - 0.10). Obviously the longer PLL-205 000 complexed by PVS, was less flexible in the texturized groove compared to the shorter PLL-25 700, which was able to adopt a less constrained orientation.

Therefore to validate the effect and check for a systematic trend or functional relation further PLL samples with the varying M_w = 3 400, 20 700, 57 900, 80 000, 189 400, 246 000, 309 500 g/mol) were used and deposited consecutively with PVS. Analogously the corresponding order parameters were determined for those PEMs. The result is given in Figure 6a, where the order parameters S are plotted versus the molecular weight (M_w) of all PLL samples. A significant increase of order is seen with increasing M_w. Hence, systematically the longer PLL rods showed the higher alignment in the surface grooves than the smaller ones, which were not influenced by the confined space. For a deeper understanding the theoretically approximated contour lengths L of the different α-helical PLL samples were plotted against the experimentally determined opening angles γ of the rod

assembly, which is shown in Figure 6b. For the calculation of the approximate contour lengths $L_{PLL\text{-}3.400}$ - $L_{PLL\text{-}309.500}$ the degree of polymerisation (DP) and the known rise per residue of r = 0.15 nm for the α-helix[26] were used according to L = DP * r.

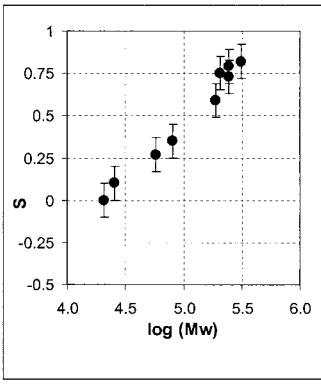

Figure 6a. (partially data from [9] with kind permission of ACS) Dependence of the order parameter S on the molecular weight (M_w) of PLL in PEM-5 consecutively adsorbed with PVS at texturized Si substrates.

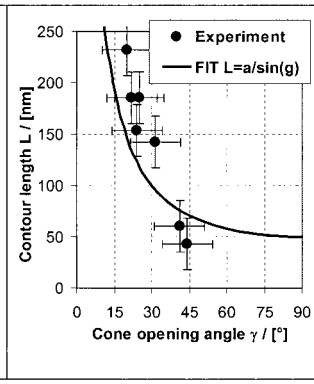

Figure 6b. Relation between the contour length L of various PLL samples and the cone opening angle γ due to Equation (5). The analytical function (6) was used.

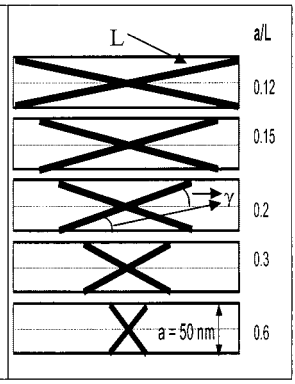

Figure 6c. Scheme of the confinement effect of a surface groove (width a) on the alignment of stiff polymer rods (contour length L). Only two rods of an assumed bundle are shown.

The following simple geometrical model was applied to represent the experimental data,

$$a/L = \sin(\gamma) \tag{6}$$

considering the contour length L as the hypothenusis and a, the groove width, as the opposite cathete of a triangle (Figure 6c). a was the optimised parameter in that approach resulting in a = 50±10 nm. This was quite consistent with the average width of the surface grooves found by AFM.[9] In Figure 6c a scheme on the confinement effect of nanoscopic surface grooves on rod alignment is shown. With these data it can be shown that α-helical PLL form rods in PEMs (i), that their degree of alignment scales with their varying contour length (ii) and that the ratio between groove width a and contour length L is obviously the determining factor for orientation in PEMs of α-PLL/PVS (iii). Arguments for the PLL alignment within surface grooves are currently under discussion with several working groups. Suggestions for main driving forces of PLL rods to confine within the surface grooves and not to exceed the groove space are:[9]

-The higher population of reactive geminal Si-OH groups due to mechanical scratching causes more surface contacts with the α-helical polypeptides, especially PLL compared to the non-groove region.

-The ammonium groups of α-helical PLL rods can form ion pairs not only with the surface charges at the bottom but also with those at the side walls of the groove (half cylinder). Therefore charged rods might form more surface contacts, if they are surrounded by groove walls compared to facing only the planar surface.

Dependence on the layer number

As a further parameter, the influence of the PEL layer number on the unidirectional alignment of PLL rods within the PEM-1 to PEM-5 was studied. As a result in the Figure 7 the order parameter S of PLL-246.800 based on the Amide II band is plotted against the adsorption step z = 1 to 5 of PEM-PLL/PVS-z.

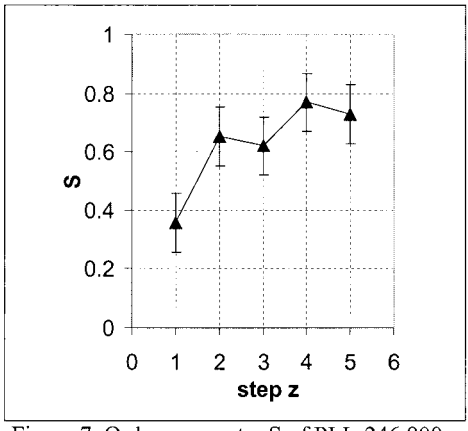

Figure 7. Order parameter S of PLL-246.800 in PEM-z of PLL/PVS in the presence of 1 M $NaClO_4$ in dependence of the layer number z.

An increase from the first PLL layer (PEM-1) from S = 0.36 to S = 0.73 for the the last PLL layer (PEM-5) was observed and it seemed that PEM-z with z > 5 would reach a constant value between S = 0.7 - 0.8. This demonstrates that there is a correlation between the number of assemblied PLL rods within the nano grooves and the degree of alignment. Assuming triangular or even conical shape of the surface grooves PEMs might grow from both the bottom and the side walls to fill the empty space. Hence possibly, the more PLL rods are assembled under complexation with the polyanions, the smaller gets the available space in the

grooves, which might enhance the PLL alignment with respect to the groove direction. Furthermore in Figure 7 a modulating course in the order parameter was observed, so that after each polyanion step S is slightly increased compared to the one before. This might be interpreted as a compacting and orienting effect of the outermost polyanion layer onto the underlying PLL rods.

Microscopic characterization (AFM)

In the preceding section it was shown, that the internal structure of PEMs of PLL/PVS exhibited a high degree of orientation induced by parallel surface textures. Hence, it was interesting, how the surface morphology of those thin film assemblies looks like. This was checked by AFM measurements (tapping mode) on the dry PEM sample. In Figure 8a an AFM picture on the PEM-5 of PLL-246.500/PVS, consecutively deposited on a texturized silicon substrate, is given.

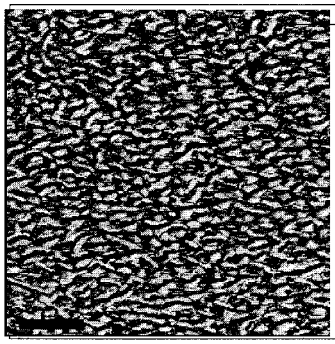

Figure 8a. AFM picture of a PEM-5 composed of PLL-246.500/PVS. The graph scales with 5 x 5 micron (height x width). (texture direction lies parallel to the scaling bar (left), which corresponds to 1 μm).

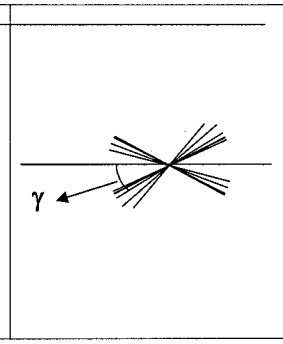

Figure 8b. Texture vectors of worm-like objects found in Fig. 7a due to oriented nanoscopic complexes of PLL/PVS shifted to the same origin of a double cone with opening angle $\gamma = 30°$.

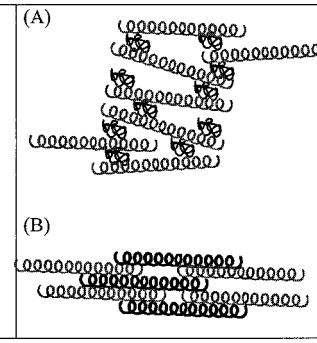

Figure 8c. (A) Proposed model for PEMs of stiff α-helical PLL and coiled PVS (similar to [9] with kind permission of ACS)
(B) Proposed model for PEM consisting of α-helical PLL and α-helical PLG (description in the chapter 2).

A nano-structured surface morphology giving hints for anisotropically oriented elements (white coloured ´worms´) with dimensions of about 200 nm is visible. This might be attributed to partially aligned aggregated PLL/PVS complex moieties. For various of such aligned worm-like objects in the graph texture vectors were drawn, which all had certain inclinations from the texture direction. Recombining them to one center, a double cone could be obtained, which is shown in Figure 8b. Analogously to the orientation model used in FTIR spectroscopy an opening angle of $\gamma = 30°$ of that double cone could be determined, which is in approximate agreement with the opening angle obtained by ATR-FTIR $\gamma = 22°$ for the same PLL-246.500 sample. Although the length scales of these two experiments are different, principles of self similarity might prevail. Hence, the larger scaled surface structures seen by AFM might be related to the lower scaled molecular dimensions, which were probed by IR spectroscopy.

Model

Conclusively in Figure 8c a scheme for the internal structure of PEMs of PLL/PVS is proposed. The layered lammellar structure might be valid in the horizontal as well as in the vertical direction of the PEM. In principle PLL forms the α-helical rods (grey) by specific interaction of the bulky ClO_4^- anions with the polypeptide backbone inserting within the charged ammonium groups of PLL[27] Hence, charged α-helical polypeptides like PLL show an ´anti-polyelectrolyte´ behavior, since they stretch upon salt addition. Whereas, PVS itself shows the classical polyelectrolyte behavior: it forms coils (black) due to the charge screening by the high salt content (1 M $NaClO_4$). Complexing these two PELs supramolecular assemblies are suggested consisting of PLL rods, which are oriented in the case of a texturized (command) surface and PVS coil, which form a kind of glue between the PLL rods.

2. PEM of PLL/PLG

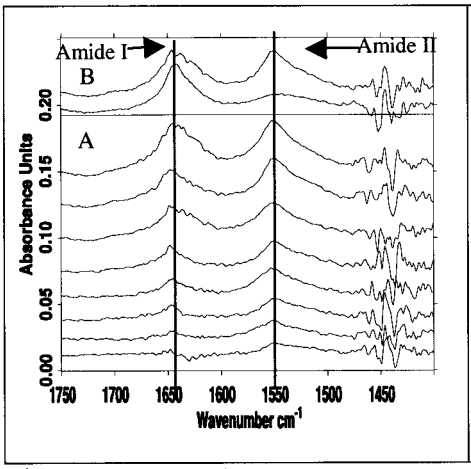

Figure 9a. (A) p-polarized ATR-FTIR spectra on the consecutive deposition of PLL and PLG from $NaClO_4$ solutions in dependence of the adsorption step z = 1 to 8 (from bottom to top). (B) The two uppermost spectra are due to the p- and s-polarized spectrum of PEM-8 of PLL/PLG in the presence of 1 M $NaClO_4$.

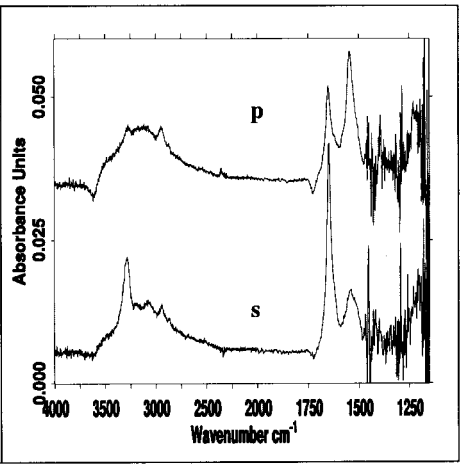

Figure 9b. p- and s-polarized ATR-FTIR spectra of the PEM-8 of PLL/PLG in the dry state after rinsing with water and drying by N_2 flow.

As it was pointed out above, PEMs of PLL/PVS consist of stiff α-helical PLL and coiled PVS. Consequently, PEMs of two stiff α-helical polypeptides shall be introduced asking on their orientation features. Hence, here we report some preliminary results on the PEM system consisting of PLL and PLG, being both in the α-helical state. In the Figure 9a related *in-situ*-ATR FTIR spectra on the consecutive deposition of PLL/PLG from $NaClO_4$ containing solutions are shown. From the increasing signals of the Amide I band at 1 647 cm^{-1} and of the Amide II band at 1 550 cm^{-1}, the successful built up of PEM-1 to PEM-8 can be proven. Generally for that specific system we only see an overlap of the amide bands from PLL and from PLG. However, since in these spectra the Amide I and Amide II bands did not show significant wavenumber changes upon consecutive adsorption of PLL and PLG, both polypeptides appear to be in the α-helical state. Furthermore, the p- and s-polarized spectra of the PEMs ending either with the PLL or with the PLG component show a high dichroic ratio of $R_Y^{ATR} > 3.0$ with repect to the Amide II band (upper part B) suggesting high order parameters S, which are given in the Table 2.

Additionally the effect of drying was addressed at. For that the spectra of PEM-8 in the dry state are shown in the full range in Figure 9b, in which additionally also the Amide A band (ν(NH)) could be evaluated, since for the dry case this band does not suffer from interferences with the ν(OH) band. The resulting R_y^{ATR} values are summarized in Table 2, whereby for the sake of comparison only the Amide II band was considered.

Table 2. Dichroic ratios R^T, order parameter S and opening angle γ for PEMs of PLL/PLG (based on the Amide II band).

	PLL-309.500 / PLG-70.000			
Amide II	PEM-6, wet	PEM-7, wet	PEM-8, wet	PEM-8, dry
R^T	3.33	4.5	3.63	2.41
S	0.58	0.75	0.63	0.58
γ	32°	24°	30°	32°

From the order parameters $S \geq 0.6$ for the dry as well as the wet state a high unidirectional orientation could be concluded for both the α-helical PLL as well as the α-helical PLG rods, which is based on the average of both spectroscopically undistinguishable polypeptide orientations. A slight increase of alignment was obtained for the PLL terminated PEM (PEM-7) in comparison to the PLG terminated one (PEM-6, PEM-8). Furthermore, drying of the PEM-8 did not change the polypeptide alignment in the wet state, which was also observed for PEMs composed of PLL and a flexible polyanion earlier.[8] Conclusively, based on the high order parameter for both stiff compounds (PLL and PLG) a structural model for such PEMs is given in the Figure 8c (B) suggesting parallel (lammelar) oriented rods of both α-heli-cal PLL and α-helical PLG. Whereas the α-helical conformation of PLL was expected due to the specific PLL/ClO_4^- interaction, this was surprising for PLG, since it is not known that PLG forms the α-helix in 1 M $NaClO_4$ solutions. Hence, it can be speculated if α-helical PLL rods might induce the α-helix of PLG by the exact matching of the opposite charges or by dipole/dipole interaction. Microscopic investigations on this system are currently under way.

3. PEM of PANI/polyanion

Based on the the high macromolecular order observed in the reported PEMs composed of stiff α–helical polypeptides, further synthetic stiff PELs came into consideration asking if they can be oriented in an analogous manner. Interesting macromolecular compounds with this respect

are conductive polymers, since they are charged and expected to be stiff in their doped form. Conductive polymers are commonly known to be poorly soluble in water at pH = 7, to have poor film forming capabilities and to be poorly processable in melts. Hence, to circumvent the first two difficulties, the multilayer technique was applied to immobilize conductive polymers from aqueous solutions, which was initially shown by Rubner and coworkers for polypyrrole (PPY) and polyaniline (PANI).[28, 29, 30]

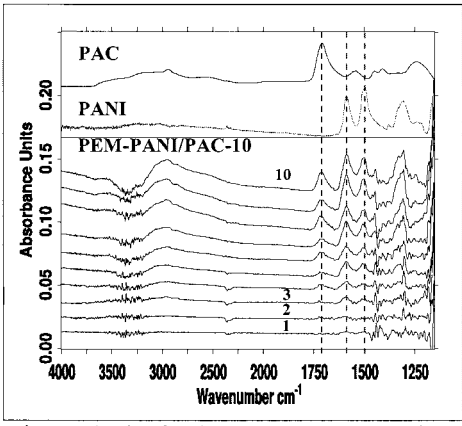

Figure 10a. in-situ ATR-FTIR spectra on the consecutive deposition of PEM-10 consisting of PANI/PAC (from bottom to top: PEM-1 - PEM-10).

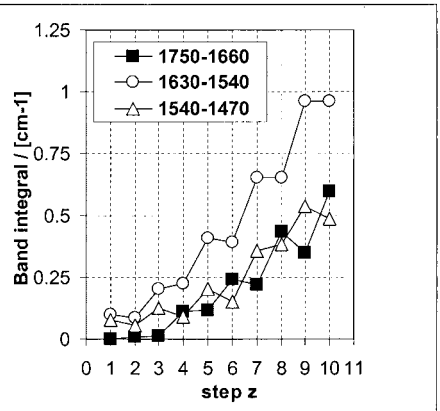

Figure 10b. Adsorbed amount versus adsorption step rationalized by the integrated band areas of the ν(C=O) (1750-1660 cm^{-1}) of PAC and the ν(C=C) of the aromatic/chinoidic structures of PANI (1630-1540, 1540-1470 cm^{-1}).

Referring to that studies and in order to exploit our spectroscopic analytical capabilities, doped PANI was consecutively adsorbed in alternating steps with PAC, where acidic PANI solutions of water and NMP (9:1 v/v) were used. As preliminary results in-situ-ATR-FTIR spectra on the consecutive deposition of PANI/PAC at texturized silicon crystals are shown in Figure 10a. From the increasing intensities of IR bands due to PANI and to PAC film formation and growth could be concluded. This is quantitatively shown in Figure 10b, where the integrated band areas of the ν(C=O) of PAC and the ν(C=C) due to the chinoid (1 630-1 540 cm^{-1}) and benzeneoid (1 540-1 470 cm^{-1}) structures of PANI are shown. Interestingly, with every PAC step slight amounts of PANI were removed from the previous PEM. With that we could show that our analytical approach was valid to prove consecutive PANI/PAC deposition.

Moreover, analogously to the polypeptide PEMs we were interested, whether the surface texture had any orientation effect on PANI layers. Up to now applying again dichroic ATR-

FTIR spectroscopy, we could not obtain dichroic effects similar to the polypeptide PEMs. Hence for the moment no alignment of the PANI within the PEM was concluded for that particular system. In future different experimental parameters will be varied to achieve alignment of PANI.

Conclusion

- PEMs consisting α-helical PLL and optionally PVS (i) or α-helical PLG (ii) were deposited at substrates texturized by parallel nanoscopic surface grooves and studied by dichroic ATR-FTIR spectroscopy.
- From the dichroic ratios of the amide bands order parameters $S \geq 0.6$ were obtained suggesting a significant alignment of charged α-helical polypeptides in PEMs containing PLL/PVS (i) as well as PLL/PLG (ii).
- For the PEM consisting of PLL/PVS (i) the deposited amount as well as the order parameter S were significantly dependent on the molecular weight (contour length) of PLL and the opening angle γ of a model cone consisting of α-helical PLL rods was proven to be a function of both contour length and width of the confining surface grooves.
- Models consisting of rods and coils (PLL/PVS) (i) and exclusively of rods (PLL/PLG) (ii), respectively, were concluded from the obtained data.
- AFM pictures on PEM-PLL/PVS showed anisotropically oriented worm-like structures
- Multilayers of conductive PANI alternating with PAC could be successfully deposited. No alignment of PANI could be obtained by the texturized substrate up to now.

Acknowledgement

We thank the Deutsche Forschungsgemeinschaft (DFG) for financial support (SFB 287, B5).

[1] G. Decher, J. D. Hong and J. Schmitt, *Thin Solid Films* **1992**, *210/211*, 831.
[2] A. S. Michaels, R. G. Miekka, *J. Phys. Chem.* **1961,** *65* (10), 1765.
[3] V. A. Kabanov, *Polymer Science*, **1994**, *36*, 2.
[4] G. Decher, *Science* **1997**, 1232.
[5] M. Castelnovo, J. F. Joanny, *Langmuir* **2000**, *16*(19), 7524.
[6] E. R. Kleinfeld, G. S. Ferguson, *Science* **1994**, 265, 370.
[7] X. Arys, A. Laschewsky, A.M. Jonas, *Macromolecules* **2001,** *34*, 3318.
[8] M. Müller, *Biomacromolecules* **2001**, 2(1), 262.
[9] M. Müller, B. Kessler, K. Lunkwitz, *J. Phys Chem. B* **2003,** *107* (in press).
[10] C. Picart, P. Lavalle, P. Hubert, F. J. G. Cuisinier, G. Decher, P. Schaaf, J. C. Voegel, *Langmuir* **2001,** *17*(23), 7414.
[11] P. Lavalle, C. Gergely, F. J. G. Cuisinier, G. Decher, P. Schaaf, J. C. Voegel, C. Picart, *Macromolecules* **2002**, *35*(11), 4458.

[12] F. Boulmedais, P. Schwinte, C. Gergely, J.C. Voegel, P. Schaaf, *Langmuir* **2002**, *18*(11), 4523
[13] P. Schwinte, J.C. Voegel, C. Picart, Y. Haikel, P. Schaaf, B. Szalontai, *J. Phys. Chem. B* **2001**, *105*(47), 11906
[14] J. Chluba, J.C. Voegel, G. Decher, P. Erbacher, P. Schaaf, J. Ogier, *Biomacromolecules* **2001**, *2*(3), 800
[15] P. Schwinte, V. Ball, B. Szalontai, Y. Haikel, J.C. Voegel, P. Schaaf, *Biomacromolecules* **2002**, *3*(6), 1135
[16] L. Richert, P. Lavalle, D. Vautier, B. Senger, J.F. Stoltz, P. Schaaf, J.C. Voegel, C. Picart, *Biomacromolecules* **2002**, *3*(6), 1170
[17] M. Müller (in preparation)
[18] U.P. Fringeli, in *'Encyclopedia of Spectroscopy and Spectrometry'*, J.C. Lindon, G.E. Tranter, J.L. Holmes (eds), Academic Press, 2000
[19] M. Müller, T. Rieser, K. Lunkwitz, S. Berwald, J. Meier-Haack, D. Jehnichen, *Macromol. Rapid Commun.* **1998**, *19*(7), 333
[20] M. Müller, in *'Handbook of Polyelectrolytes and Their Applications'*, Eds. S.K. Tripathy, J. Kumar, H. S. Nalwa, Vol. 1, American Scientific Publishers (ASP), 2002, pp. 293-312
[21] N.A. Nevskaya and Y.N. Chirgadze, *Biopolymers* **1976**, *15*, 637
[22] R. Zbinden, *IR-Spectroscopy of High Polymers*, Academic Press, NY 1964
[23] U.P. Fringeli, M. Schadt, P. Rihak, Hs. H. Günthard, *Z. Naturforsch.* **1976**, *31a*, 1098
[24] J. Michl and E.W. Thulstrup, Spectroscopy with polarized light, VCH Publishers, New York 1986
[25] T. Miyazawa, *J. Chem. Phys.*, 32, 1647 (1960) &. S. Krimm, *J. Mol. Biol.* **1962**, *4*, 528
[26] G.E. Schulz, R.H. Schirmer, Principles of protein structure, Springer, N.Y, 1985
[27] G. Ebert und Y.-H. Kim, *Progr. Colloid & Polymer Sci.*, **1983**, *68*, 113
[28] A.C. Fou and M.F. Rubner, *Macromolecules* **1995**, *28*, 7115
[29] J.H. Cheung, M*acromolecules* **1997**, *30*, 2712
[30] W.B. Stockton and M.F. Rubner, *Macromolecules* **1997**, *30*, 2717